CORTEX 72 (2015) 168–178

Available online at www.sciencedirect.com

ScienceDirect

Journal homepage: www.elsevier.com/locate/cortex

Special issue: Research report

Specificity of V1–V2 orientation networks in the primate visual cortex

Anna W. Roe [a,b,*] *and Daniel Y. Ts'o* [c,1]

[a] *Department of Psychology, Vanderbilt University, Nashville, USA*
[b] *Zhejiang University Interdisciplinary Institute of Neuroscience and Technology, Zhejiang University, Hangzhou 310027, China*
[c] *Department of Neurosurgery, SUNY-Upstate Medical University, Syracuse, NY, USA*

ARTICLE INFO

Article history:
Received 13 January 2015
Reviewed 31 March 2015
Revised 7 July 2015
Accepted 7 July 2015
Published online 22 July 2015

Keywords:
Orientation selectivity
Optical imaging
Cross correlation
Cortico–cortical connectivity
V1
V2

ABSTRACT

The computation of texture and shape involves integration of features of various orientations. Orientation networks within V1 tend to involve cells which share similar orientation selectivity. However, emergent properties in V2 require the integration of multiple orientations. We now show that, unlike interactions within V1, V1–V2 orientation interactions are much less synchronized and are not necessarily orientation dependent. We find V1–V2 orientation networks are of two types: a more tightly synchronized, orientation-preserving network and a less synchronized orientation-diverse network. We suggest that such diversity of V1–V2 interactions underlies the spatial and functional integration required for computation of higher order contour and shape in V2.

1. Introduction

Orientation networks within V1 are embodied within horizontal networks of anatomical patches (Malach, Amir, Harel, & Grinvald, 1993; Sincich & Blasdel, 2001) whose cells share similar orientation selectivity (Ts'o, Gilbert, & Wiesel, 1986). Such networks are viewed as the first step towards the generation of visual object shape recognition. Area V2 is distinguished from V1 by its generation of higher properties that enable it to encode orientation selectivity independent of specific inducing cue orientation or cue type. These inferred contours include occluded contours or illusory contours (von der Heydt & Peterhans, 1989; Ramsden, Hung, & Roe, 2001, 2014), motion contrast borders (Lu et al., 2010; Rasch et al., 2013), disparity capture borders (Bakin, Nakayama, & Gilbert, 2000), texture borders (Merigan, Nealey, & Maunsell, 1993), and borders inferred from colinearity or other complex shapes (Gilad, Meirovithz, Leshem, Arieli, & Slovin, 2012; Hegde & Van Essen, 2000). Furthermore, some higher order orientation

* *Corresponding author*. Oregon Health & Sciences University in Portland, Oregon, USA.
E-mail addresses: annawang@zju.edu.cn (A.W. Roe), dan@tsolab.org (D.Y. Ts'o).
[1] Tel.: +315 464 5531; fax: +315 464 5504.
http://dx.doi.org/10.1016/j.cortex.2015.07.007

selective cells are specific to cue type (e.g., illusory contours), whereas others appear to be invariant across different types of cues (e.g., orientation tuned regardless of inducer cue type) (Ramsden et al., 2014). These emergent contour recognition properties in area V2 suggest an integration, either directly or indirectly, across multiple oriented inputs from V1 and a diversity of functional interactions between V1 and V2. However, to date, there is little understanding regarding the relationship of oriented responses in V1 with those in V2.

In this study, using optical imaging and cross correlation methods, we examine the functional relationships between orientation-selective cells in V1 and V2. By examining similarity of orientation selectivity and degree of receptive field (RF) overlap, we find evidence for two types of V1–V2 orientation networks. The relationship of these findings to previous anatomical and functional studies of V1–V2 connectivity is discussed.

2. Results

Our data set consists of 76 oriented–oriented V1–V2 cell pairs (subsequently referred to as 'oriented cell pairs') identified out of entire population of 273 V1–V2 cell pairs. Cross-correlograms were computed from the stimulated activity of these cell pairs, shuffled-corrected and normalized. The distribution of peak heights was then divided into quartiles, creating four peak strength categories (0, 1, 2, 3), corresponding to flat or weak correlations (0–1), and moderate to strong correlations (2–3) (see Methods and Roe & Ts'o, 1999). Of these, 34 cell pairs were of peak strength 2–3. Numbers of cell pairs are shown in Table 1. 130 V2–V2 and 336 V1–V1 correlograms were also collected for comparison. All cell pairs included in this study were recorded on separate electrodes, and confined to the superficial cortical layers (a laminar dependence of V1/V2 correlations has been reported, Smith, Jia, Zandvakili, & Kohn, 2013). For each correlogram, we used peak height as a measure of interaction strength, peak width as a measure to temporal dispersion of spike firing coincidence, and peak position (offset from exact coincidence: 0 msec) as a measure of relative V1–V2 timing.

Within the distances sampled (0–4°), we found no significant relationship between peak height and RF separation for the overall population (V1–V2 $r^2 = .0085$, V2–V2 $r^2 = .0133$) or for any of the subpopulations in this study. Thus, differences in peak characteristics were not due to effect of RF separation. For most analyses, we focused on correlograms with moderate to strong peaks (peak strength 2 or 3) because we could interpret the peak positions and widths of strong peaks with greater confidence.

Table 1 – Number of V1–V2 cell pairs.

	All	Peak 2 or 3
Total	273	133
All oriented–oriented	76	34
Similarly oriented	30	17
Differently oriented	46	22
Broadband oriented-broadband oriented	28	13
Color oriented-color oriented	40	19
Total nonoriented–nonoriented	102	60

2.1. General characteristics of V1–V2 correlograms

Fig. 1 illustrates a few examples of correlograms obtained from oriented V1–V2 cell pairs. Typical of V1–V2 correlograms, they have broad peaks in comparison to V1–V1 correlograms. A range of dependencies on spatial overlap and orientation matching was observed (see Fig. 1). Both cell pairs shown in Fig. 1A and B share similar orientations and have strong peak strengths even though there is RF overlap in 1A but not 1B. However, RF overlap without matched orientation can also result in strong interaction peaks (Fig. 1C). High RF overlap does not always predict strong correlation (Fig. 1D). Thus, strong interactions between oriented cell pairs can occur with (Fig. 1A, C) or without (Fig. 1B) RF overlap and with similar (Fig. 1A, B) or different (Fig. 1C) orientation selectivities. We then examined the prevalence of these characteristics within the population.

2.2. Peak width: V1–V2 temporal dispersion

To measure the extent of temporal dispersion in V1–V2 interactions (that is, tightness of synchronization between two cells), we examined the peak width of the correlogram Narrow peaks imply a smaller degree of jitter in relative spike timing, whereas broad peaks indicate a large distribution of spike coincidences.

As shown in Fig. 2A, the peak widths of the V1–V2 correlograms (blue bars) are typically 5–50 msec wide (average = 28.0 msec). This is similar to the distribution of V2–V2 peak widths (red bars, mean = 21.0 msec), but is much broader than that of V1–V1 peaks (yellow bars, mean = 3.9 msec). Thus, on average V1–V2 and V2–V2 peak widths are at least several times broader than V1–V1 peak widths, indicating that V1–V2 and V2–V2 interactions are more temporally dispersed than V1–V1 interactions.

Fig. 2B illustrates the peak width distribution of oriented V1–V2 correlograms. The peak widths of oriented cell pairs are similar in breadth to the overall V1–V2 population; 90% of the widths fell between 5 and 50 msec (oriented–oriented mean = 19.3 msec, all pairs mean = 28.0, $p < .002$). The primary difference is that more oriented cell pairs (39%) had narrow 5–10 msec widths than in the overall population (18%) ($p < .002$). Oriented V1–V2 peak widths are broader than those of V1–V1 cell pairs, and do not differ from oriented V2–V2 cell pairs (mean = 16.6 msec, $p > .2$, not shown).

2.3. Peak height: oriented cell pairs have smaller peaks

The histology stain for cytochrome oxidase (CO) has helped define several important functional subcompartments and pathways in V1 and V2. The V1 interblob-V2 pale/thick stripe pathway has been shown to contain a prominence of non-color selective (broadband) oriented cells, whereas the V1 CO blob-V2 thin stripe pathway contains a prominence of color selective, non-oriented cells (Hubel & Livingstone, 1987; Landisman & Ts'o, 2002a, 2002b; Levitt, Kiper, & Movshon, 1994; Livingstone & Hubel, 1984; Roe & Ts'o, 1995, 1999; Ts'o

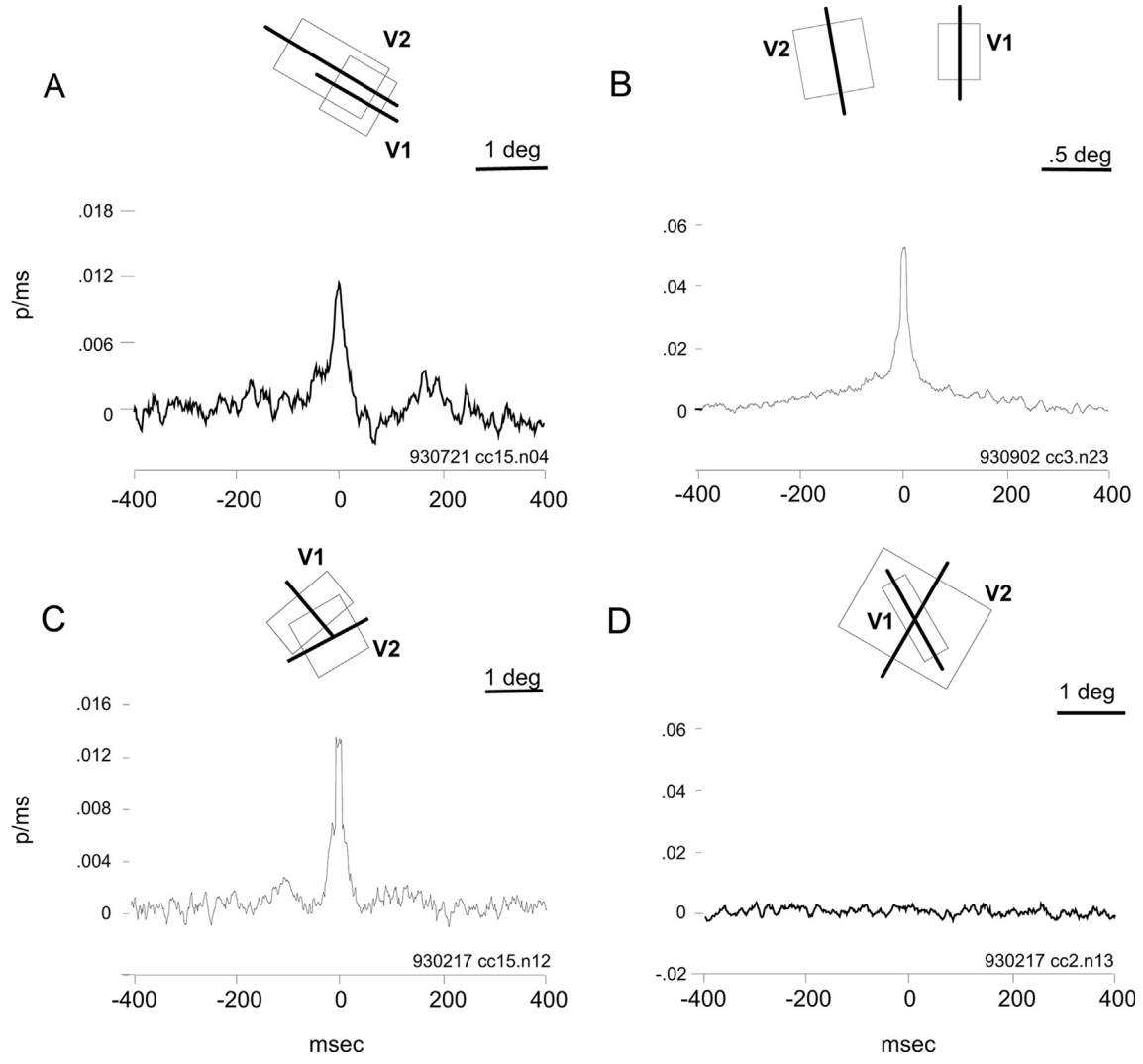

Fig. 1 – Examples of oriented V1–V2 cell pairs. Receptive fields and orientations indicated by rectangles and and central lines, respectively. Temporal coincidence on ordinate (msec). Likelihood of occurrence (probability per msec) on abscissa. A) Cell pair with similar orientation selectivities (0° diff) and 50% RF overlap. RF separation .3°. B) Cell pair with similar (20° diff) orientation selectivities and 0% receptive field overlap. RF separation 1.3°. C) Cell pair with dissimilar (95° diff) orientation selectivities and 45% RF overlap. Rf separation .75°. D) Cell pair with dissimilar (60° diff) orientation selectivities and 100% RF overlap. RF separation .1°.

and Gilbert, 1988). To examine whether these two parallel V1–V2 systems are distinguishable with respect to their functional interactions, we made two comparisons: oriented versus non-oriented V1–V2 cell pairs and broadband oriented versus color non-oriented V1–V2 cell pairs.

As shown in Fig. 3A, oriented–oriented cell pairs (blue dots, mean width = 19.3 msec, mean height = .0125) had significantly narrower and smaller peaks than non-oriented/non-oriented cell pairs (pink open dots, mean width = 28.5 msec, mean height = .0164) (width $p < .008$, height $p < .003$). A similar dichotomy exists between broadband oriented (Fig. 2B, blue dots) and color-selective non-oriented (Fig. 3B, pink open dots) cell pairs (width $p < .02$, height $p < .05$). These differences in peak height and peak width are not related to differences in RF separation ($p > .1$). These results suggest that V1–V2 interactions between oriented cells are weaker than those between non-oriented cells.

2.4. *Importance of RF overlap*

We previously reported that RF overlap is important for some classes of V1–V2 color cells but not others (Roe & Ts'o, 1999). To examine whether interactions between oriented cell pairs require RF overlap, we examined peak height for overlapped and non-overlapped cell pairs. We found that overlapped RFs ($n = 37$) had significantly stronger peaks than non-overlapped ($n = 39$) ($p < .001$). As shown in Fig. 4A, over 70% of non-overlapped cell pairs had weak or flat correlogram peaks (Peak 0/1), while over 60% of overlapped cell pairs had moderate or strong peaks [Peak 2/3; $\chi^2(.999) = 15.25$, df = 3].

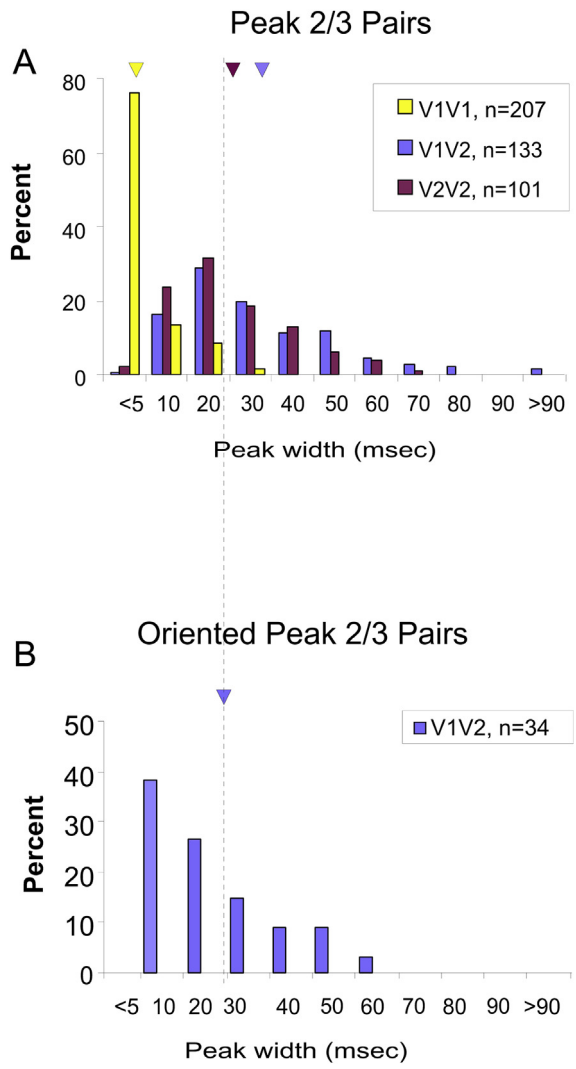

Fig. 2 – V1–V2 peak width (at half height) distributions. Only strong peaks (Peak 2/3) are shown. Bin 10 indicates all values > 5 msec and ≤10 msec; Bin 20 indicates all values > 10 msec and ≤20 msec. Means are indicated by arrowheads at top of graph. A) Peakwidth distributions of V1–V1 (yellow, mean = 3.9 msec), V1–V2 (blue, mean = 28.0 msec), and V2–V2 (red, mean = 21.0 msec) cell pairs. Dashed vertical line denotes mean of oriented–oriented V1–V2 peak widths (below) for comparison. B) Distribution of oriented–oriented V1–V2 peak widths (Peak 2/3, mean = 19.3 msec).

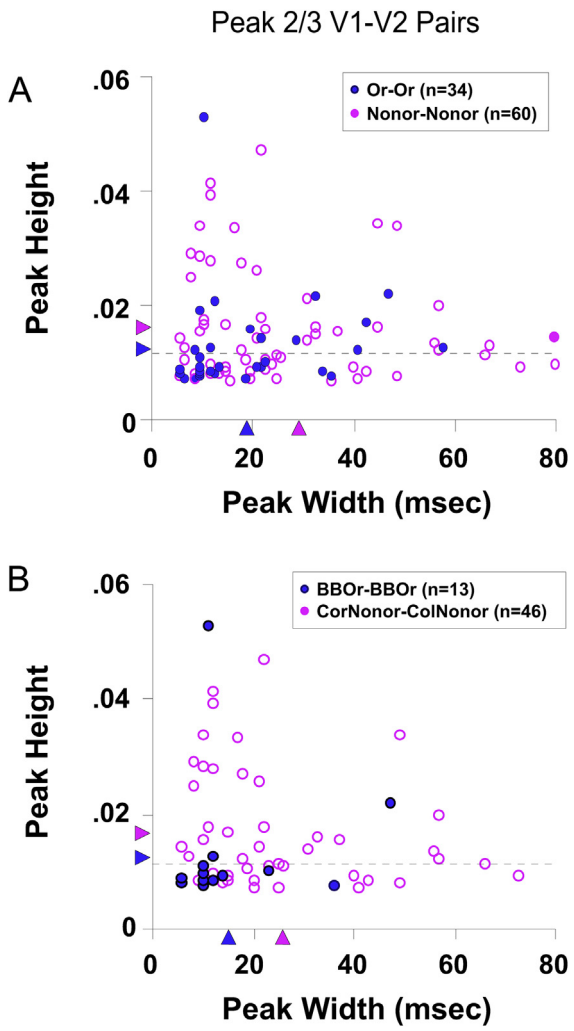

Fig. 3 – Oriented V1–V2 cell pairs have weaker interactions than non-oriented V1–V2 cell pairs. Peak 2/3 cell pairs are shown. Dotted horizontal lines indicate cutoff value for strongest (Peak 3) peaks. A) Oriented cell pairs have narrower peak widths (blue dots, mean = 19.3 msec) than non-oriented (pink dots, mean = 28.5 msec) cell pairs ($p < .008$). They also have significantly smaller peak heights (oriented height mean = .0125, non-oriented height mean = .0164, $p < .003$). Solid pink dot has actual peak width of 137 msec and peak height of .0144. B) Broadband oriented pairs (blue dots, mean = 15.9 msec) have narrower peak width than color non-oriented (pink dots, mean = 24.6 msec) cell pairs ($p < .02$). They also have smaller peak height [broadband oriented mean = .0135; color non-oriented mean = .0171, $\chi^2(.95) = 4.54$, df = 1].

This dependency on RF overlap was not related to orientation similarity. As shown in Fig. 4B, for cell pairs with matched orientation (diff ≤ 30°, $n = 30$), non-overlapped RFs tended to have weak interactions (76% = 13/17) and overlapped RFs strong interactions (62% = 8/13) [$\chi^2(.9) = 7.15$, df = 3]. Similarly, for cell pairs with non-matched orientation (diff > 30°, $n = 46$), non-overlapped RFs tended to have weak interactions (68% = 15/22) and overlapped RFs strong interactions (63% = 15/24) [$\chi^2(.99) = 10.9$, df = 3]. Thus, both pairs with matched orientation and those with non-matched orientation selectivity exhibit a dependency on RF overlap. Such dependency on RF overlap implies that orientation interactions between V1 and V2 occur over limited spatial extents. This is in sharp contrast to color–color interactions (Roe & Ts'o, 1999).

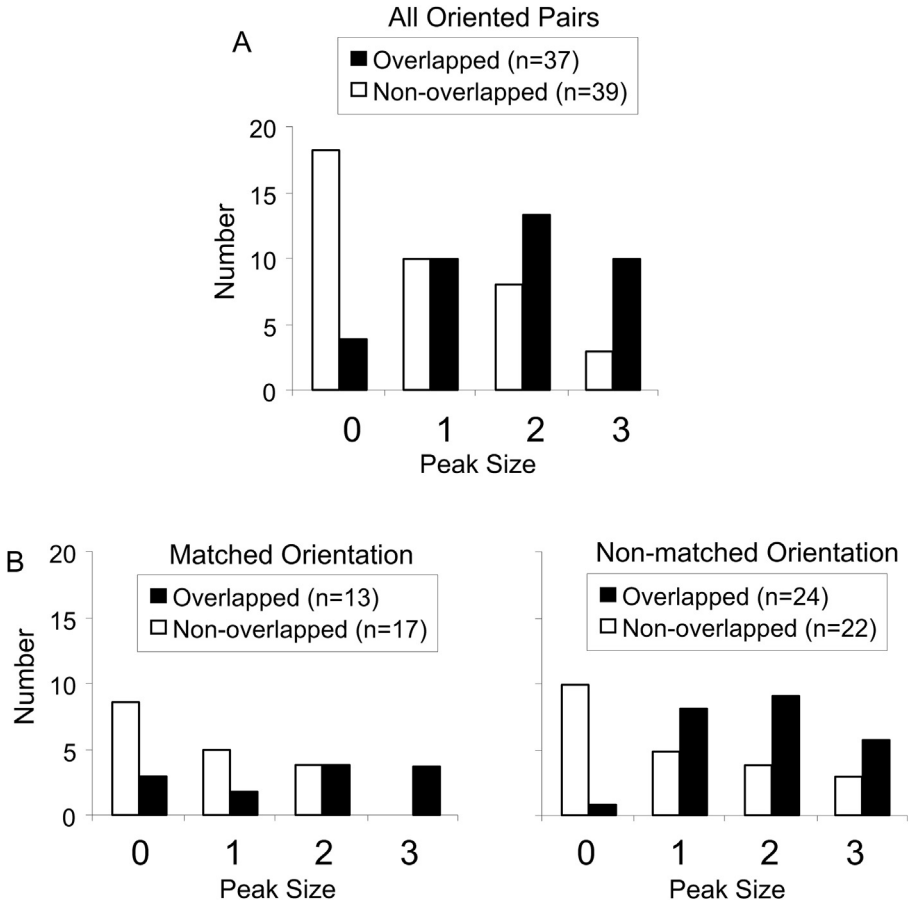

Fig. 4 – Importance of receptive field overlap. A) Overlapped oriented cell pairs ($n = 37$) had significantly stronger peak heights than non-overlapped cells pairs ($n = 39$). B) Both matched orientation (left) and non-matched orientation (right) cell pairs exhibit dependency on receptive field overlap.

2.5. *Peak position*

Given the hierarchical positions of V1 and V2 (Felleman & Van Essen, 1991) and their relative latency distributions (Girard, Hupe, & Bullier, 2001; Munk, Nowak, Girard, Chounlamountri, & Bullier, 1995; Nowak, Munk, Girard, & Bullier, 1995; Schroeder, Mehta, & Givre, 1998), one might predict a greater number or a greater strength of feedforward than feedback interactions. As shown below, this hierarchical relationship between V1 and V2 is reflected in interaction strength and not in the numbers of feedforward versus feedback interactions.

2.5.1. *Feedforward interactions are stronger than feedback*

Consistent with previous reports, the position of many V1–V2 correlogram peaks are centered on zero, indicating a significant amount of common input to V1–V2 cell pairs (Fig. 5A). Peak positions of the large majority (92%) fall between −7 msec and +7 msec, with half (55%) falling between −2 msec and +2 msec. Although positive (presumptive feedforward) and negative (presumptive feedback) peak positions are equally numerous, there is a tendency for peaks with positive position (mean = .0158) to be stronger than those with negative (mean = .0129, $p < .025$). This distinction is even more apparent for oriented cell pairs (Fig. 5B). Here, we see that the strongest peaks (peak 3) are mostly feedforward (positive position points in large gray rectangle to right). This is true for both pairs with similar orientations (3 out of 4, pink dots) and with different orientations (7 out of 9, blue dots). However, moderate sized peaks (peak 2) are mostly feedback (points in smaller gray rectangle to left). Thus, strong V1–V2 coactivation is coupled with a tendency for feedforward interactions to be stronger than feedback.

2.5.2. *No dependence of peak height on orientation similarity*

To examine whether similarity of orientation-selectivity is also a determinant of interaction strength, we examined the matched (≤30° orientation difference) and non-matched (>30° orientation difference) populations. One expectation might be that V1–V2 cell pairs with matching orientation exhibit stronger correlation peaks than non-matching cell pairs.

Contrary to expectations, as shown in Fig. 5B, both orientation matched ($n = 12$) and non-matched ($n = 22$) populations exhibited a similar range of interaction strengths; there was no significant difference in their peak strengths ($p > .3$). RF separations for matched ($n = 12$, mean = .6°, range .5–1.3°) and non-matched ($n = 22$, mean = .6, range = .5–1.3) pairs

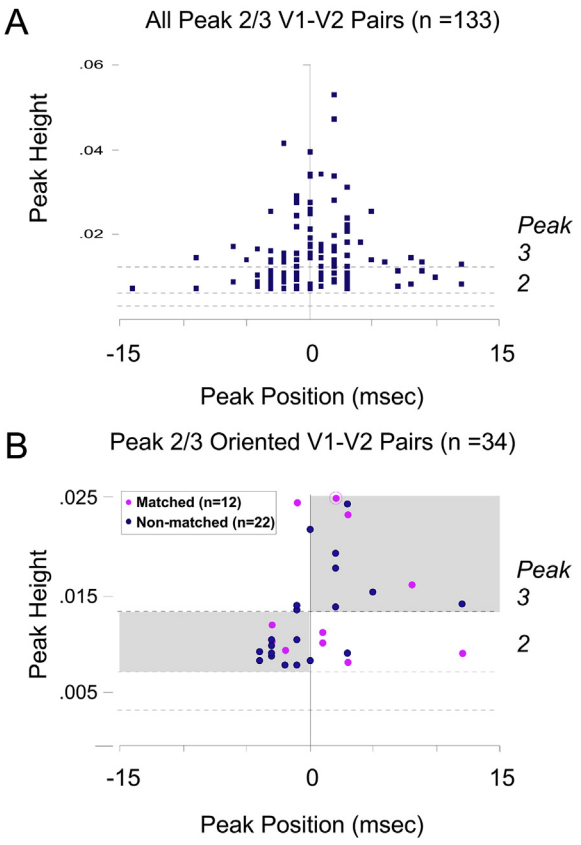

Fig. 5 – Peak height versus peak position. Positive peak position indicates V1–V2 feedforward interaction; negative peak position indicates V2–V1 feedback interaction. Horizontal dotted lines demarcate divisions between Peak Strengths 0, 1, 2, and 3. A) Most V1–V2 peaks are centered on zero. Feedforward interactions tend to be stronger. B) Matched (pink dots) and non-matched (blue dots) oriented pairs have similar peak strengths. Stronger interactions are feedforward (Peak 3, points falling in large gray rectangle) and weaker interactions are feedback (Peak 2, points falling in smaller gray rectangle). Note that some points overlap and appear as single points. Circled pink dot has a peak position of +2 msec and a peak height of .053.

were not different ($p > .3$). We next asked whether, for cell pairs that have overlapped RFs, orientation similarity might increase interaction strength. After separating the population of overlapped cell pairs into orientation matched and non-matched groups, we found no difference in peak height distribution (matched, $n = 13$, mean = .0114; non-matched, $n = 24$, mean = .0090, $p > .3$). Neither did non-overlapped cell pairs, separated into orientation matched and non-matched populations, exhibit any differences in peak height (similar mean = .0045, different mean = .0056, $p > .05$). Thus, for either overlapping or non-overlapping oriented cell pair populations, adding the criterion of orientation similarity does not increase interaction strength as measured by peak height.

2.5.3. *Peak position: possible difference in feedforward/feedback interaction strengths or orientation matched versus non-matched cell pairs*

Another point that can be observed from Fig. 5B is that for cell pairs with different orientation (blue dots), most (12 out of 13) of the moderate peak (peak 2) oriented cell pairs exhibited feedback interactions. Thus, although our sample size is limited, these comparisons suggest a dichotomy in the strength of feedforward versus feedback interactions. First, feedforward interactions (both orientation matched and non-matched) are stronger than feedback (most peak 3 pairs have positive peak positions). And second, most feedback interactions in the moderate interaction strength category (peak 2) occur between orientation non-matched cell pairs.

2.6. *Peak width: dependence on orientation matching*

Although we found no difference in peak height for similarly preferring versus dissimilarly oriented cell pairs, we did find differences in peak width. As shown in Fig. 6A, orientation matched cell pairs (mean = 13.1 msec, $n = 30$) had narrower peak widths than non-matched cell pairs (mean = 20.2 msec, $n = 46$) [χ^2 (.9) = 12.0, df = 7; $p < .02$]. This also holds for the subset of color oriented-color oriented cell pairs (Fig. 6B, non-matched: $n = 23$, mean = 27.0 msec; matched: $n = 17$, mean = 11.8 msec, $p < .004$). Non-color selective (broadband) oriented-broadband oriented cells also showed a similar tendency (Fig. 6C), but this difference did not reach significance, probably because of small sample size (All pairs: matched, $n = 8$, mean = 11.6 msec; non-matched: $n = 20$, mean = 16.8 msec, $p > .1$). Thus, some difference in temporal dispersion of coincidence exists between oriented cell pairs with similar and with different orientations.

3. Discussion

3.1. *Summary*

We report here that oriented V1–V2 cell pairs exhibit a significant degree of specificity. In contrast to V1–V1 correlograms, V1–V2 peaks are several times broader and are not necessarily dependent on orientation similarity. In contrast to non-oriented cell pairs, V1–V2 oriented interactions are weaker and spatially dependent. Oriented V1–V2 cell pairs can further be separated into orientation-preserving and orientation-diverse networks.

Fig. 7A summarizes the relative peak heights and widths of different V1–V2 cell pairs. These 'average' correlograms illustrate that, of the interactions examined, interactions between color non-oriented cell pairs (red line) are the strongest and those between oriented cell pairs (blue and black lines) the weakest. In addition, as shown in (Roe & Ts'o, 1999), average interactions between color non-oriented V1 cells and oriented V2 cells are of intermediate size (green line). Although orientation-matched (black line) and orientation-nonmatched (blue line) interactions are of equal strength, non-matched interactions exhibit more temporal scatter (broader peaks). Below, we discuss the interpretation of these

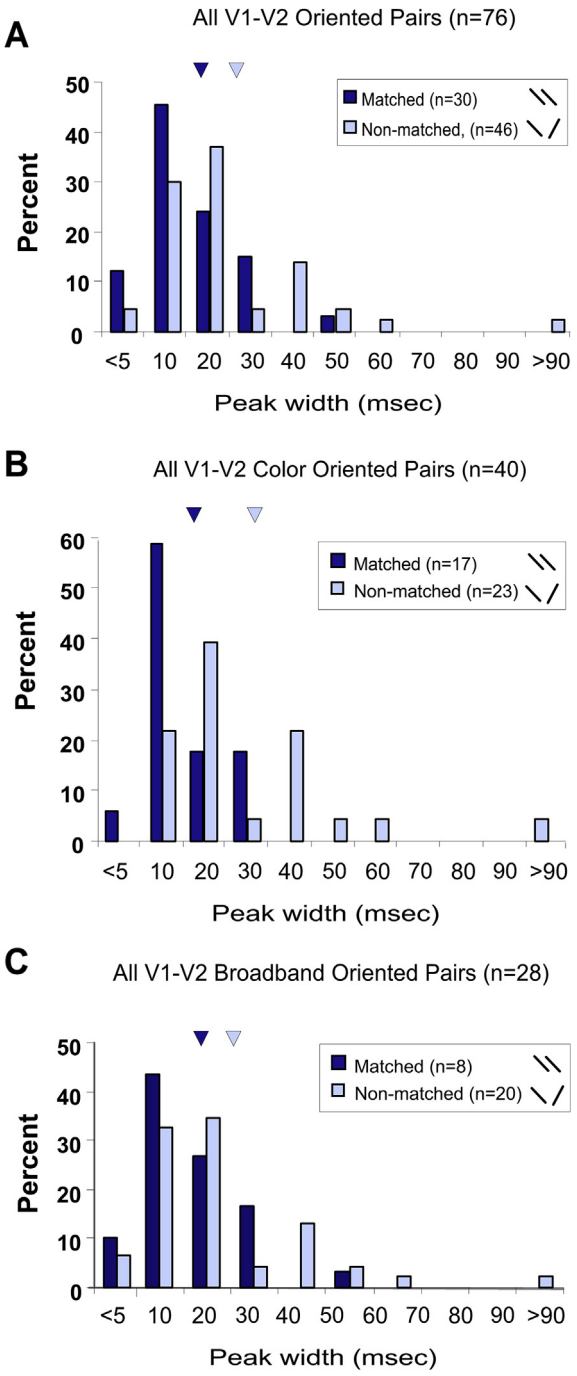

Fig. 6 – Matched orientation cell pairs have narrower peak widths than non-matched pairs. Matched orientation (dark blue bars, ≤30° difference), non-matched orientation (light blue bars, >30° difference). A) All oriented–oriented cell pairs. Matched: n = 30, mean = 13.1. Non-matched: n = 46, n = 20.2 ($p < .02$). B) Color oriented-color oriented cell pairs. Matched: n = 17, mean = 11.8. Non-matched: n = 23, n = 27.0 ($p < .004$). C) Broadband oriented-broadband oriented cell pairs (n = 28). Matched: n = 8, mean = 11.6. Non-matched: n = 20, mean = 16.8 ($p > .1$).

relative peak heights and widths, especially with regard to network size.

3.2. *Peak height and peak width as an indicator of network size*

Peak height is a measure of the maximal capability (under a specific context) of a cell to fire within a fixed temporal offset to another. Thus peak height is an indication and measure of interaction strength. Peak width is an indicator of temporal dispersion in relative spike firings, and, in principle, is independent of peak height. One can have large number of coincidences that are tightly (narrow tall peak) or loosely correlated (broad tall peak), or a small number of coincidences that are tightly (narrow low peak) or loosely correlated (low broad peak). That they are independent measures in this data set is supported by the poor correlation between peak height and peak width of V1–V2 cell pairs ($r^2 = .03$).

Why does one cell pair fire in a temporally dispersed manner and another pair with a fairly fixed temporal coincidence? Synaptic strength is one obvious answer, as broad peaks could indicate that individual connectivities are relatively ineffective. Another possibility is the specific network configuration. Other factors such as bursting can also lead to a broadening of peak widths (Nowak & Bullier, 2000; van Vreeswijk & Hansel, 2001). In addition, network size (number of neurons) also contributes to peak width. A cell that is influenced by only one other cell is likely to have much tighter temporal correlation (i.e., narrower peak) than a cell that is influenced by 100 other cells and even more so than a cell that is influenced by 10,000 other cells. So to the extent that it is more probable that two cells in a large network will have greater temporal correlation dispersion, peak width may be indicative of network size. We will focus our discussion below on possible relationship of peak width to network size, which may not necessarily refer to the anatomical network but rather the currently active functional network.

3.3. *V1–V2 networks are larger and less synchronized than V1–V1 networks*

The breadth of V1–V2 peaks could indicate that, relative to V1–V1 interactions, individual V1–V2 connectivities are relatively less effective and/or that there are many more cells contributing to the spike firing of the V2 cell (i.e., a larger network). Anatomically, V1–V2 connections are much more spatially convergent and divergent than those in V1. Whereas lateral horizontal connections within the superficial layers of V1, as studied with anatomical tracers, extend up to only 2 mm from an injection site (Blasdel, Lund, & Fitzpatrick, 1985; Gilbert & Wiesel, 1979; Malach et al., 1993; Rockland, 1985; Sincich & Blasdel, 2001), feedforward and feedback projections are highly divergent (Livingstone & Hubel, 1984; Sincich & Horton, 2002a, 2002b; Ts'o, Roe, & Gilbert, 2001; Weller & Kaas, 1983). Indeed, individual V1–V2 and V2–V1 arbors can extend as much as 3–4 mm (Rockland & Virga, 1989, 1990), converging onto single loci in V2 (Livingstone & Hubel, 1984; Sincich & Horton, 2002a, 2002b; Ts'o et al., 2001). In addition, intrinsic V2–V2 connections extend for several millimeters and are well poised to mediate V1 influences on

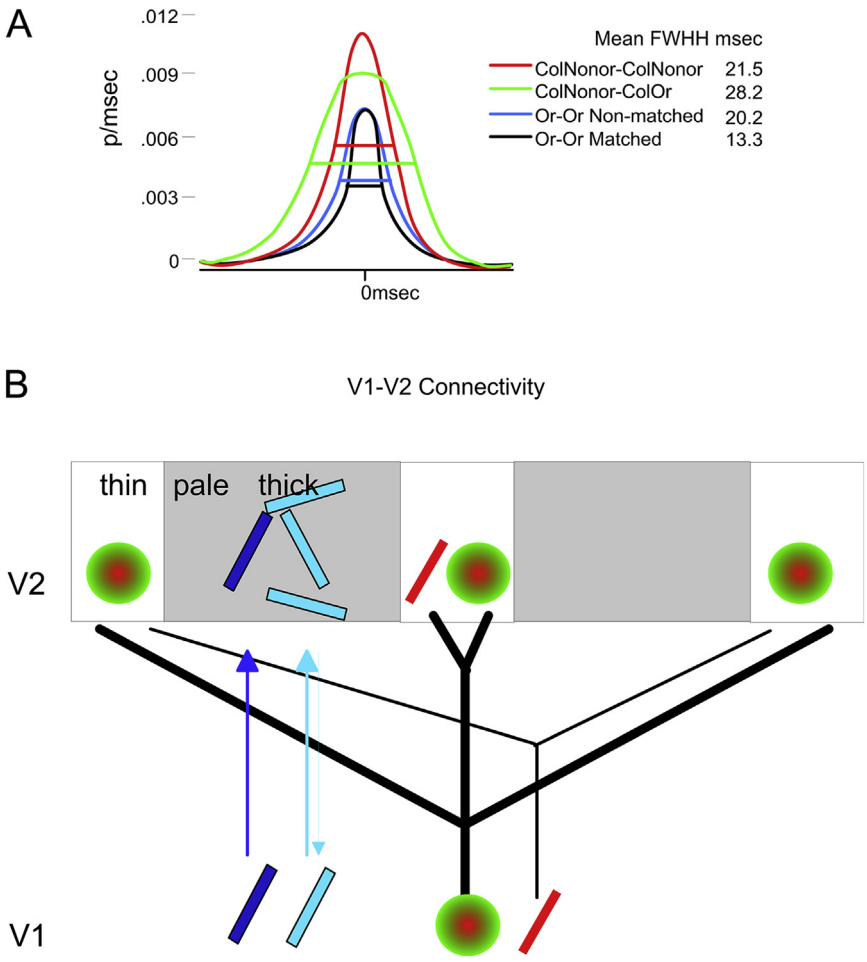

Fig. 7 – Summary of V1–V2 interactions. A) Average correlograms for different populations of V1–V2 cell pairs, and their mean full width at half height (FWHH) in msec. Color-nonoriented/color-nonoriented (red, n = 80, mean height = .115, mean width = 21.5 msec), color-nonoriented/color-oriented (green, n = 30, mean height = .0090, mean width = 28.2 msec), non-matched oriented–oriented (blue, n = 46, mean height = .0074, mean width = 20.2 msec), and matched oriented–oriented (black, n = 30, mean height = .0080, mean width = 13.1 msec). On average, interactions between color non-oriented cell pairs are strongest and those between oriented cell pairs weakest. B) Schematized V1–V2 networks. Interactions between some types of color cells do not require receptive field overlap and occur over large spatial extents (12). These include non-oriented color cell pairs (schematized by red/green disks) and oriented V1 (red bar)-nonoriented V2 cell pairs. In contrast, oriented interactions (blue bars) between V1 and V2 are spatially specific (depend on receptive field overlap). Two orientation-selective networks are suggested: one orientation-preserving (dark blue) and another orientation-diverse (light blue). Prevalence of feedback interactions for orientation-diverse network is depicted by light blue feedback arrow.

distant locations in V2 (Levitt, Yoshioka, & Lund, 1994; Malach et al., 1993; Rockland, 1985). This anatomical convergence and divergence suggests that V1–V2 networks may involve more neurons than V1–V1 networks (Budd, 1998). Thus, the finding that V1–V2 correlogram peaks are considerably broader than V1–V1 peaks is consistent with a larger neuronal network of V1–V2 than V1–V1 interactions.

3.4. *Larger non-oriented networks, smaller orientation-selective networks*

Several studies exist that have identified the CO stripe location of anatomical tracer injection sites within V2 (Livingstone & Hubel, 1984; Sincich & Horton, 2002a, 2002b). Careful examination of these studies suggests that thin stripe injections label a larger area of V1 than pale/thick stripe injections. From measurements taken from Figs. 25–28 in Livingstone and Hubel (1984) and Fig. 2 in Sincich and Horton (2002a) and Fig. 5 in Sincich and Horton (2002b), thin stripe injections produced labeled area of patches in V1 measuring 5 mm, 6 mm, and >5 mm in extent, and pale stripe injections resulted in labeled V1 regions 3 mm, 3.5 mm, 4.5 mm, 4.5 mm in size, and one thick stripe injection resulted in labeled V1 interblob regions 3 mm in size. Differences in labeled area did not appear to be due to differences in injection site. Furthermore, this is consistent with the observation that layer 2/3 neurons

in V1 project to only a single pale stripe (Federer, Williams, Ichida, Merlin, & Angelucci, 2013). Thus, these anatomical observations are consistent with our findings that oriented interactions are weaker (Fig. 2) and more spatially restricted (Fig. 4) than non-oriented interactions (Roe & Ts'o, 1999). We suggest that large, less synchronous non-oriented networks are consistent with their role in the encoding of surface properties (such as brightness and color), whereas greater temporal and spatial synchrony may be required for the computation of contours.

3.5. *Larger orientation-diverse networks, smaller orientation-preserving networks*

We observe that correlogram peaks of orientation-matched pairs have similar heights but narrower peaks than orientation-nonmatched interactions. This suggests that both populations have similar interaction strengths, but, as discussed above, may participate in different sized networks. We discuss possible roles of a smaller stimulus-preserving network and a slightly larger stimulus-diverse network.

On a local scale it is important to compute orientation accurately and to localize its position precisely in visual space. These are functions that V1 is capable of performing (Vogels, 1990). However, to compute, for example, the orientation of inferred contours is a much more complex process requiring both specific integration and generalized outcome (Gove, Grossberg, & Mingolla, 1995; Peterhans & von der Heydt, 2001). In the computation of curvature and shape (Hegde & Van Essen, 2000), where nearby points on a curve share the same orientation and distant points on a curve may have quite different orientations, different modes of orientation integration may also be required. Multiple orientation networks may also be tied to multiple orientation domains in V2, some of which are V1-like and others which respond to a combination of lower and higher order contours (Ramsden et al., 2014). Thus, multiple contour processing networks between V1 and V2 may serve to preserve local contour information and at the same time produce emergent transformations that are a hallmark of contour processing in V2.

The present study did not systematically attempt to present stimulus configurations designed to trigger V2 contour processing per se, or evoke binding between disparate stimulus elements. Such stimuli have been proposed to elicit increases in gamma band synchrony, which in turn has been shown to strengthen intracortical and V1–V2 cortico-cortical coupling (Jia, Tanabe, & Kohn, 2013). We might expect that using such stimuli would tap into specific correlational networks that are also specific to particular V2 functional subcompartments.

3.6. *Relationship to the two pale stripe system*

Orientation selective cells lie primarily within the thick and pale stripes of V2, which receive inputs from interblob regions of V1 (Livingstone & Hubel, 1984; Sincich & Horton, 2002a). Pale stripes are further distinguished into two types (Federer et al., 2009, 2013; Felleman et al., 2014; Roe & Ts'o, 1995; Shipp & Zeki 2002). Pale stripes associated with thick stripes (lying lateral to thick stripes, Type II) receive input from layer 4B in V1, exhibit greater orientation selectivity, smaller RFs with smaller scatter, and larger orientation domains with smoothly changing orientation preference across the stripe. Those associated with thin stripes (lying lateral to thin stripes, Type I) do not receive input from layer 4B in V1, exhibit lower orientation selectivity and greater color selectivity, larger receptive size and scatter, and smaller orientation domains and maps with rapidly changing orientation preference. Thick stripes are heterogeneous and contain functional domains selective for ocular disparity (Chen, Lu, & Roe, 2008), lower and higher order contour orientation selectivity (Chen et al., 2014; Pan et al., 2012; Ramsden et al., 2001, 2014), and motion contrast borders (Chen et al., 2014; Lu, Chen, Tanigawa, & Roe, 2010). They have direct projections to MT (Born & Bradley, 2005; DeYoe & Van Essen, 1985; Shipp & Zeki, 1985, 1989) and likely indirect projections to V4 (Ninomiya, Sawamura, Inoue, & Takada, 2011), and thus have strong ties with both the dorsal and ventral pathways.

This dichotomy raises the possibility that the orientation matched V1–V2 networks are associated with the thick/pale stripe system and the orientation non-matched V1–V2 networks are associated with the thin/pale stripe system. This interesting possibility will require future studies.

3.7. *A role of feedback in dissimilar orientation interactions?*

Although V1–V2 interactions are predominantly centered on zero, indicating prevalence of common input (see Nowak & Bullier, 2000), the strongest interactions are feedforward while moderate-sized interactions are feedback (Fig. 5). Although our sample size is not large, we find it notable that many of the orientation-nonmatched interactions are feedback interactions (represented by light blue feedback arrow in Fig. 7B). This is consistent with the finding that feedback connections from V2 orientation domains distribute across a broad range of orientations in V1 (Shmuel et al., Soc Neurosci Abstr 24:767, 1998). Furthermore, some of the observed higher order, contextual effects associated with V2 feedback (Bullier, Hupé, James, & Girard, 1996; Hupe et al., 1998; Ramsden et al., 2001) are likely to involve interactions between cells of non-matching orientation.

4. Methods

4.1. *Surgical prep, optical imaging, and electrophysiology*

Nine adult monkeys (*Macaca fascicularis*) were used as described in a previous study (Roe & Ts'o, 1999). Animals were anesthetized (sodium pentothal, 1–2 mg/kg/h), paralyzed (pancuronium bromide, 100ug/kg/h) and artificially respirated. Vital signs including heartrate and EEG were continuously monitored, CO_2 was maintained at 4%, and rectal temperature at 38°. Eyes were dilated, refracted and fitted with contact lens to focus on a computer monitor. A 1 cm^2 craniotomy and durotomy were made over the lunate sulcus, and a stainless-steel chamber mounted. All procedures were conducted in accordance with NIH guidelines.

Optical imaging of intrinsic cortical signals was used to localize functional compartments within V1 and V2 (Roe &

Ts'o, 1999; Ts'o, Frostig, Lieke, & Grinvald, 1990; Roe & Ts'o, 1995). Several microelectrodes were positioned to simultaneously target CO blobs and interblobs in V1, and CO thin, pale, and thick stripes in V2. The RF locations of cell pairs were separated by at most a few degrees, which was the extent of spatial representation in our craniotomies (typically 8 mm × 6 mm at 3–5° eccentricity).

RFs were plotted and qualitatively characterized. Orientation-selectivity was rated on a qualitative scale (see Livingstone & Hubel, 1984; Roe & Ts'o, 1999): A (<30° total width), B (<60°), C (<120°), to D (non-oriented), and only cells with A or B orientation sharpness were considered "oriented". Color selectivities were determined by using narrow band interference filters ranging from 450 to 630 nm. Further details of neuron classification are provided in Roe and Ts'o (1999).

4.2. *Spike train collection and cross correlation analysis*

Following isolation and characterization, neural spike trains were collected. Because of the low spontaneous firing rates typical of cortical neurons, we collected spike trains in response to visual stimulation. Both cells were stimulated simultaneously with bars (optimal orientation and color) moving in synchrony across each RF. Spike trains and stimulus sync pulses were recorded and time stamped (temporal resolution .1 msec). Post-stimulus time histograms and raw cross correlograms were calculated.

We used shuffle subtraction methods to minimize stimulus-induced increases in correlation (Brody, 1999; Nowak, Munk, James, Girard, & Bullier, 1999; Nowak, Munk, Nelson, James, & Bullier, 1995; Perkel, Gerstein, & Moore, 1966). Correlograms (computed at ±400 msec, 1.6msec binwidths and ±50 msec, .1 msec binwidths) were normalized for spike firing rate [1/sqrt(numspike1*numspike2)] and smoothed (weighted, moving Gaussian average 7 bins). Peak position, peak height, and peak widths (at half-height) were determined. Only peaks at least 2 standard deviations above baseline were considered for peak analysis. Our data set peak values ranged from 0 to .05. The dataset was divided into quartiles and indexed from 0 to 3, yielding four peak strength categories (Roe & Ts'o, 1999). RF separation was defined as center-to-center distance. RF overlap is defined as max[% RF(i) overlapping RF(j)]. Statistical comparison of distributions was evaluated with student's *t*-test unless otherwise indicated.

Acknowledgments

We thank Lara Hinderstein and Carmela LoRusso for excellent technical support, Ben Ramsden, Rob Friedman, and Barbara Heider for helpful comments on manuscript. Supported by EY06347, EY08240, EY11744 and the Whitaker Foundation.

REFERENCES

Bakin, J. S., Nakayama, K., & Gilbert, C. D. (2000). Visual responses in monkey areas V1 and V2 to three-dimensional surface configurations. *Journal of Neuroscience, 20*, 8188–8198.

Blasdel, G. G., Lund, J. S., & Fitzpatrick, D. (1985). Intrinsic connections of macaque striate cortex: axonal projections of cells outside lamina 4C. *Journal of Neuroscience, 5*, 3350–3369.

Born, R. T., & Bradley, D. C. (2005). Structure and function of visual area MT. *Annual Review of Neuroscience, 28*, 157–189.

Brody, C. D. (1999). Correlations without synchrony. *Neural Computation, 11*, 1537–1551.

Budd, J. M. (1998). Extrastriate feedback to primary visual cortex in primates: a quantitative analysis of connectivity. *Proceedings of the Royal Society of London B Biological Sciences, 265*, 1037–1044.

Bullier, J., Hupé, J. M., James, A., & Girard, P. (1996). Functional interactions between areas V1 and V2 in the monkey. *Journal of Physiology (Paris), 90*, 217–220.

Chen, G., Lu, H. D., & Roe, A. W. (2008). A map of horizontal disparity in primate V2. *Neuron, 58*, 442–450.

Chen, M., Li, P., Zhu, S., Han, C., Xu, H., Fang, Y., et al. (2014). An orientation map for motion boundaries in macaque V2. *Cerebral Cortex*.

DeYoe, E. A., & Van Essen, D. C. (1985). Segregation of efferent connections and receptive field properties in visual area V2 of the macaque. *Nature, 317*(6032), 58–61.

Federer, F., Ichida, J. M., Jeffs, J., Schiessl, I., McLoughlin, N., & Angelucci, A. (2009). Four projection streams from primate V1 to the cytochrome oxidase stripes of V2. *Journal of Neuroscience, 29*, 15455–15471.

Federer, F., Williams, D., Ichida, J. M., Merlin, S., & Angelucci, A. (2013). Twoprojection streams from macaque V1 to the pale cytochrome oxidase stripes of V2. *Journal of Neuroscience, 33*, 11530–11539.

Felleman, D. J., Lim, H., Xiao, Y., Wang, Y., Eriksson, A., & Parajuli, A. (2014). The representation of orientation in macaque V2: four stripes not three. *Cerebral Cortex*.

Felleman, D. J., & Van Essen, D. C. (1991). Distributed hierarchical processing in the primate cerebral cortex. *Cerebral Cortex, 1*, 1–47.

Gilad, A., Meirovithz, E., Leshem, A., Arieli, A., & Slovin, H. (2012). Collinear stimuli induce local and cross-areal coherence in the visual cortex of behaving monkeys. *PLoS One, 7*(11), e49391.

Gilbert, C. D., & Wiesel, T. N. (1979). Morphology and intracortical projections of functionally characterised neurones in the cat visual cortex. *Nature, 280*, 120–125.

Girard, P., Hupe, J. M., & Bullier, J. (2001). Feedforward and feedback connections between areas V1 and V2 of the monkey have similar rapid conduction velocities. *Journal of Neurophysiology, 85*, 1328–1331.

Gove, A., Grossberg, S., & Mingolla, E. (1995). Brightness perception, illusory contous, and corticogeniculate feedback. *Visual Neuroscience, 12*, 1027–1052.

Hegde, J., & Van Essen, D. C. (2000). Selectivity for complex shapes in primate visual area V2. *Journal of Neuroscience, 2*, RC61–RC66.

von der Heydt, R., & Peterhans, E. (1989). Mechanisms of contour perception in monkey visual cortex. I. Lines of pattern discontinuity. *Journal of Neuroscience, 9*, 1731–1748.

Hubel, D. H., & Livingstone, M. S. (1987). Segregation of form, color, and stereopsis in primate area 18. *Journal of Neuroscience, 7*, 3378–3415.

Hupe, J. M., James, A. C., Payne, B. R., Lomber, S. G., Girard, P., & Bullier, J. (1998). Cortical feedback improves discrimination between figure and background by V1, V2 and V3 neurons. *Nature, 394*, 784–787.

Jia, X., Tanabe, S., & Kohn, A. (2013). Gamma and the coordination of spiking activity in early visual cortex. *Neuron, 77*, 762–774.

Landisman, C. E., & Ts'o, D. Y. (2002a). Color processing in macaque striate cortex: relationships to ocular dominance, cytochrome oxidase, and orientation. *Journal of Neurophysiology, 87*, 3126–3137.

Landisman, C. E., & Ts'o, D. Y. (2002b). Color processing in macaque striate cortex: electrophysiological properties. *Journal of Neurophysiology, 87*, 3138–3151.
Levitt, J. B., Kiper, D. C., & Movshon, J. A. (1994). Receptive fields and functional architecture of macaque V2. *Journal of Neurophysiology, 71*, 2517–2542.
Levitt, J. B., Yoshioka, T., & Lund, J. S. (1994). Intrinsic cortical connections in macaque visual area V2: evidence for interaction between different functional streams. *Journal of Comparative Neurology, 342*, 551–570.
Livingstone, M. S., & Hubel, D. H. (1984). Anatomy and physiology of a color system in the primate visual cortex. *Journal of Neuroscience, 4*, 309–356.
Lu, H. D., Chen, G. C., Tanigawa, H., & Roe, A. W. (2010). A motion direction map in macaque V2. *Neuron, 68*(5), 1002–1013.
Malach, R., Amir, Y., Harel, M., & Grinvald, A. (1993). Relationship between intrinsic connections and functional architecture revealed by optical imaging and in vivo targeted biocytin injections in primate striate cortex. *Proceedings of the National Academy of Sciences of the United States of America, 90*, 10469–10473.
Merigan, W. H., Nealey, T. A., & Maunsell, J. H. R. (1993). The effects of lesions of cortical area V2 in macaques. *Journal of Neuroscience, 13*, 3180–3191.
Munk, M. H., Nowak, L. G., Girard, P., Chounlamountri, N., & Bullier, J. (1995). Visual latencies in cytochrome oxidase bands of macaque area V2. *Proceedings of the National Academy of Sciences of the United States of America, 92*, 988–992.
Ninomiya, T., Sawamura, H., Inoue, K., & Takada, M. (2011). Differential architecture of multi-synaptic geniculo-cortical pathways to V4 and MT. *Cerebral Cortex, 12*, 2797–2808.
Nowak, L. G., & Bullier, J. (2000). Cross correlograms for neuronal spike trains. Different types of temporal correlation in neocortex, their origin and significance. In R. Miller (Ed.), *Time and the brain, conceptual advances in brain research* (pp. 53–96). Harwood Academic Publishers.
Nowak, L. G., Munk, M. H. J., Girard, P., & Bullier, J. (1995). Visual latencies in areas V1 and V2 of the macaque monkey. *Visual Neuroscience, 12*, 371–384.
Nowak, L. G., Munk, M. H. J., James, A. C., Girard, P., & Bullier, J. (1999). Cross-correlation study of the temporal interactions between areas V1 and V2 of the macaque monkey. *Journal of Neurophysiology, 81*, 1057–1074.
Nowak, L. G., Munk, M. H. J., Nelson, J. I., James, A. C., & Bullier, J. (1995). Structural basis of cortical synchronization. I. Three types of interhemispheric coupling. *Journal of Neurophysiology, 74*, 2379–2400.
Pan, Y., Chen, M., Yin, J., An, X., Zhang, X., Lu, Y., et al. (2012). Equivalent representation of real and illusory contours in macaque V4. *Journal of Neuroscience, 32*(20), 6760–6770.
Perkel, D. H., Gerstein, G. L., & Moore, G. P. (1966). Neuronal spike trains and stochastic point processes. ii. Simultaneous spike trains. *Biophysical Journal, 7*, 419–440.
Peterhans, E., & von der Heydt, R. (2001). Simulation of neuronal responses defining depth order and contrast polarity at illusory contours in monkey area V2. *Journal of Computational Neuroscience, 10*, 195–211.
Ramsden, B. M., Hung, C. P., & Roe, A. W. (2001). Real and illusory contour processing in area V1 of the primate: a cortical balancing act. *Cerebral Cortex, 11*, 648–665.
Ramsden, B. M., Hung, C. P., & Roe, A. W. (2014). Orientation domain diversity in macaque area V2. *Eye and Brain, 6*, 97–112.
Rasch, M. J., Chen, M., Wu, S., Lu, H. D., & Roe, A. W. (2013). Quantitative inference of population response properties across eccentricity from motion-induced maps in macaque V1. *Journal of Neurophysiology, 109*, 1233–1249.
Rockland, K. S. (1985). A reticular pattern of intrinsic connections in primate area V2 (area 18). *Journal of Comparative Neurology, 235*, 467–478.
Rockland, K. S., & Virga, A. (1989). Terminal arbors of individual "feedback" axons projecting from Area V2 to V1 in the macaque monkey: a study using immunohistochemistry of anterogradely transported Phaseolus vulgaris-leucoagglutinin. *Journal of Comparative Neurology, 285*, 54–72.
Rockland, K. S., & Virga, A. (1990). Orgnization of individual cortical axons projecting from area V1 (area 17) to V2 (area 18) in the macaque monkey. *Visual Neuroscience, 4*, 11–28.
Roe, A. W., & Ts'o, D. Y. (1995). Visual topography in primate V2: multiple representation across functional stripes. *Journal of Neuroscience, 15*, 3689–3715.
Roe, A. W., & Ts'o, D. Y. (1999). Specificity of color connectivity between primate V1 and V2. *Journal of Neurophysiology, 82*, 2719–2731.
Schroeder, C. E., Mehta, A. D., & Givre, S. J. (1998). A spatiotemporal profile of visual system activation revealed by current source density analysis in the awake monkey. *Cerebral Cortex, 8*, 575–592.
Shipp, S., & Zeki, S. (1985). Segregation of pathways leading from area V2 to areas V4 and V5 of macaque monkey visual cortex. *Nature, 315*(6017), 322–325.
Shipp, S., & Zeki, S. (1989). The organization of connections between areas V5 and V2 in macaque monkey visual cortex. *European Journal of Neuroscience, 1*(4), 333–354.
Shipp, S., & Zeki, S. (2002). The functional organization of area V2, I: specialization across stripes and layers. *Visual Neuroscience, 19*(02), 187–210.
Sincich, L. C., & Blasdel, G. G. (2001). Oriented axon projections in primary visual cortex of the monkey. *Journal of Neuroscience, 21*, 4416–4426.
Sincich, L. C., & Horton, J. C. (2002a). Divided by cytochrome oxidase: a map of the projections from V1 to V2 in macaques. *Science, 295*, 1734–1737.
Sincich, L. C., & Horton, J. C. (2002b). Pale cytochrome oxidast stripes in V2 receive the richest projection from macaque striate cortex. *Journal of Comparative Neurology, 447*, 18–33.
Smith, M. A., Jia, X., Zandvakili, A., & Kohn, A. (2013). Laminar dependence of neuronal correlations in visual cortex. *Journal of Neurophysiology, 109*, 940–947.
Ts'o, D. Y., Frostig, R. D., Lieke, E. E., & Grinvald, A. (1990). Functional organization of primate visual cortex revealed by high resolution optical imaging. *Science, 249*, 417–420.
Ts'o, D. Y., & Gilbert, C. D. (1988). The organization of chromatic and spatial interactions in the primate striate cortex. *Journal of Neuroscience, 8*, 1712–1727.
Ts'o, D. Y., Gilbert, C. D., & Wiesel, T. N. (1986). Relationships between horizontal interactions and functional architecture in the cat striate cortex as revealed by cross-correlation analysis. *Journal of Neuroscience, 6*, 1160–1170.
Ts'o, D. Y., Roe, A. W., & Gilbert, C. D. (2001). A hierarchy of the functional organization for color, form and disparity in primate visual area V2. *Vision Research, 41*, 1333–1349.
Vogels, R. (1990). Population coding of stimulus orientation by striate cortical cells. *Biological Cybermatics, 64*, 25–31.
van Vreeswijk, C., & Hansel, D. (2001). Patterns of synchrony in neural networks with spike adaptation. *Neural Computation, 13*, 959–992.
Weller, R. E., & Kaas, J. H. (1983). Retinotopic patterns of connections of area 17 with visual areas V-II and MT in macaque monkeys. *Journal of Comparative Neurology, 220*, 253–279.